Langmuir

ARTICLE

pubs.acs.org/Langmuir

Formation of Assemblies Comprising Ru−Polypyridine Complexes and CdSe Nanocrystals Studied by ATR-FTIR Spectroscopy and DFT Modeling

Alexey Y. Koposov,[†] Thomas Cardolaccia,[§] Victor Albert,[‡] Ekaterina Badaeva,[‡] Svetlana Kilina,[‡] Thomas J. Meyer,[§] Sergei Tretiak,[‡] and Milan Sykora*[,†]

[†]Physical Chemistry & Applied Spectroscopy, Los Alamos National Laboratory, MS J567, Los Alamos, New Mexico 87545, United States

[‡]Theoretical Division, Center for Nonlinear Studies (CNLS), and Center for Integrated Nanotechnologies (CINT), Los Alamos National Laboratory, Los Alamos, New Mexico 87545, United States

[§]Solar Fuels and Next Generation Photovoltaics Center, University of North Carolina, Chapel Hill, North Carolina 27514, United States

ABSTRACT: The interaction between CdSe nanocrystals (NCs) passivated with trioctylphosphine oxide (TOPO) ligands and a series of Ru−polypyridine complexes—$[Ru(bpy)_3](PF_6)_2$ (**1**), $[Ru(bpy)_2(mcb)](PF_6)_2$ (**2**), $[Ru(bpy)(mcb)_2](BarF)_2$ (**3**), and $[Ru(tpby)_2(dcb)](PF_6)_2$ (**4**) (where bpy = 2,2′-bipyridine, mcb = 4-carboxy-4′-methyl-2,2′-bipyridine, tbpy = 4,4′-di-*tert*-butyl-2,2′-bipyridine; dcb = 4,4′-dicarboxy-2,2′-bipyridine, and BarF = tetrakis[3,5-bis(trifluoromethyl)phenyl]-borate)—was studied by attenuated total reflectance FTIR (ATR-FTIR) and modeled using density functional theory (DFT). ATR-FTIR studies reveal that when the solid film of NCs is exposed to an acetonitrile solution of **2**, **3**, or **4**, the complexes chemically bind to the NC surface through their carboxylic acid groups, replacing TOPO ligands. The corresponding spectral changes are observed on a time scale of minutes. In the case of **2**, the FTIR spectral changes clearly show that the complex adsorption is associated with a loss of proton from the carboxylic acid group. In the case of **3** and **4**, deprotonation of the anchoring group is also detected, while the second, "spectrator" carboxylic acid group remains protonated. The observed energy difference between the symmetric, ν_s, and asymmetric, ν_{as}, stretch of the deprotonated carboxylic acid group suggests that the complexes are bound to the NC surface via a bridging mode. The results of DFT modeling are consistent with the experiment, showing that for the deprotonated carboxylic acid group the coupling to two Cd atoms via a bridging mode is the energetically most favorable mode of attachment for all nonequivalent NC surface sites and that the attachment of the protonated carboxylic acid is thermodynamically significantly less favorable.

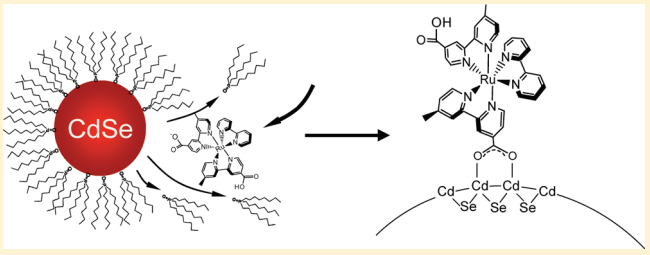

INTRODUCTION

Owing to their size-tunable electronic properties,[1] colloidal semiconductor nanocrystals (NCs) have stimulated significant interest as materials with potential to enhance performance of applications in fields such as optics, optoelectronics, photovoltaics, and others.[2] Understanding the surface chemistry of NCs is an important prerequirement for optimization of these and other emerging applications, such as chemical sensing[3] or photocatalysis.[4] In a recent study we have demonstrated that the surface passivating layer of CdSe NCs can be effectively modified, in a controlled way, with Ru−polypyridine complexes functionalized with carboxylic acid groups by a simple solution-exchange chemistry.[5] Steady-state and time-resolved photoluminescence provided insights about the dynamics of the surface exchange process and the structure of the NC−complex assembly. In the present work we focus on a more detailed understanding of the chemical interactions taking place on the surface of the NCs during the formation of NC−complex assemblies. In the experimental portion of our studies we use attenuated total reflectance FTIR (ATR-FTIR), which has been shown to be a powerful tool in studies of the surface properties of NCs.[6] Our experimental studies are complemented with density functional theory (DFT) modeling of the chemical coupling between the complexes and the NCs. This DFT modeling was recently shown to be a useful tool in studies of the interaction between semiconductor NCs and various organic ligands.[7] On the basis of results of experiment and theory, we conclude that the functionalized metal complexes attach exclusively to the cadmium sites of the NC surface via a bridging geometry, with the carboxylic acid anchoring group being deprotonated in the process.

EXPERIMENTAL SECTION

A. Materials. For the preparation of the CdSe NCs, $CdMe_2$ was purchased from Strem Chemicals; TOPO (tech grade, 90%) and TOP (tech grade, 90%) were purchased from Aldrich (Batch # 06820CH

Received: February 10, 2011
Revised: May 13, 2011
Published: May 31, 2011

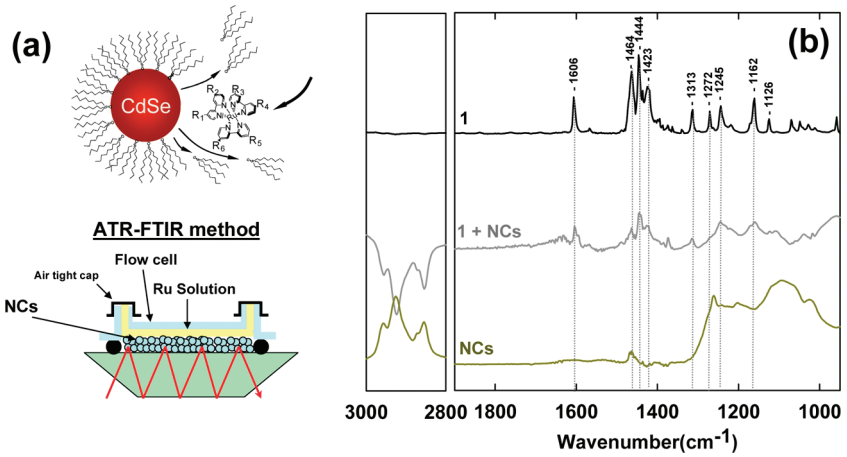

Figure 1. (a) Top: schematic diagram of the process of the Ru−polypyridine complex adsorption onto the surface of the CdSe NCs, studied in the present work. In the figure R_1 to R_6 represent various functional groups (for **1**, $R_1 = R_2 = ... = R_6 = H$). The NC and the complex are not shown in scale. Bottom: scheme of the ATR-FTIR experiment. (b) ATR-FTIR spectra of CdSe NC film following exposure to 10^{-3} M acetonitrile solution of complex **1** (traces 1 + NC). The trace shown is a difference between the spectrum recorded 60 min after exposure to the complex and several seconds after exposure to the complex. Also shown are the spectra of the independently prepared film of NCs and film of complex **1**, both measured as dry film, not exposed to the solvent.

and 07596KJ, respectively); Se shot (99.999%) was purchased from Alfa Aesar; extra dry hexane, methanol, and acetonitrile were purchased from ACROS Organics; and $[Ru(bpy)_3]Cl_2 \cdot 6H_2O$ and NH_4PF_6 were purchased from Aldrich. These chemicals were used without any purification. The complex $[Ru(bpy)_3](PF_6)_2$ (**1**) was prepared from $[Ru(bpy)_3]Cl_2 \cdot 6H_2O$ (Aldrich) by anion metathesis using a saturated aqueous solution of NH_4PF_6.[8] The complexes $[Ru(bpy)_2(mcb)](PF_6)_2$ (**2**), $[Ru(bpy)(mcb)_2](BarF)_2$ (**3**), and $[Ru(tpby)_2(dcb)](PF_6)_2$ (**4**) (where bpy = 2,2′-bipyridine, mcb = 4-carboxy-4′-methyl-2,2′-bipyridine, tbpy = 4,4′-di-*tert*-butyl-2,2′-bipyridine; dcb = 4,4′-dicarboxy-2,2′-bipyridine, and BarF = tetrakis[3,5-bis(trifluoromethyl)phenyl]borate) were prepared by methods described previously.[9] The CdSe NCs with the diameter of ∼4.0 nm (1S transition at 585 nm)[10] were prepared by established literature procedures (the full details of the synthesis were described in our recent publication).[5,11]

B. FTIR Measurements. The FTIR spectra were acquired using a Nicolet 6700 FT-IR spectrometer (Thermo Electron Inc.) equipped with an ATR accessory (PIKE Technologies). The ATR-FTIR experiments were performed in a flow cell equipped with a ZnSe ATR crystal window. To remove excess ligand, prior to the preparation of the NC films the CdSe NCs were washed twice according to standard procedure,[11] and then 1 mL of solution of nanocrystals (concentration of NQDs was $\sim 10^{-5} - 10^{-6}$ M) in hexane was drop-cast onto a ZnSe window in an inert atmosphere, and the solvent was evaporated under vacuum. The NC films were washed four times with extra dry acetonitrile. Then, the flow cell was assembled, and 1 mL of a 10^{-3} M solution of the appropriate complexes was injected into the flow cell. The flow cell was closed with airtight caps and taken out from the glovebox for measurements. The films of the complex, used as a reference, were also prepared by drop-casting of the appropriate solutions. The solutions of the deprotonated complexes were prepared by the addition of 1.2 equiv of NaOH solution in water to the solution of the appropriate complex. To ensure the full protonation of the complexes, 0.5 equiv of HPF_6 in water was added to the solution of the appropriate complex.

COMPUTATIONAL METHODOLOGY

A. Modeling of NC Structures and Ru−Polypyridine Complexes. Because of the rapidly growing computational cost with an increasing number of atoms, the quantum-chemical simulations are typically performed on NCs significantly smaller than those used in experimental studies ($d \sim 4.0$ nm). Although, as shown in many experimental and theoretical studies, the electronic structure of NCs is strongly dependent on size, in the absence of steric constraints the NC−ligand interactions are expected to be size independent. This is supported by recent computational studies of small clusters[7,12] and crystal planes[13] passivated with TOPO ligands, which indicate that the ligand binding energies do not change with NC size. Here we focus on the $Cd_{33}Se_{33}$ cluster with $d \sim 1.3$ nm, which roughly corresponds to the smallest CdSe NCs prepared experimentally.[14] Previous studies found that this cluster is one of the "magic size" structures, which are formed by a closed shell of atoms and, thus, have an exceptionally high stability.[14,15] Our cluster has been initially constructed on a wurtzite lattice with bulk Cd−Se bond lengths and then relaxed to its lowest energy configuration (see computational results section).

The metal complexes functionalized with carboxylic acid groups were modeled as acetic acid (CH_3COOH) or acetate (CH_3COO^-). We found that in the geometry-optimized structure the mode of attachment depends on the choice of the ligand starting position with respect to the surface of the $Cd_{33}Se_{33}$, resulting in either chelating or bridging binding. To determine relative strength of the attachment by these two modes, the binding energies (E_b's) for all nonequivalent binding sites (see Results and Discussion) were calculated. The E_b's were calculated as the difference between the total energies of the cluster with the adsorbed ligand, the bare optimized cluster, and an isolated optimized ligand. All structures were verified to be the true minima on the potential energy surface by harmonic frequency calculations.

B. Quantum-Chemical Methodology Used for Calculations of the Electronic Structure. The optimal geometries and electronic structure of $Cd_{33}Se_{33}$ cluster with adsorbed acetate or acetic acid have been obtained using DFT with the hybrid B3LYP functional and the LANL2DZ basis set as implemented in the Gaussian 09 software package.[16] Our previous study showed that such combination of the functional and the basis set adequately describes a small CdSe cluster passivated with common ligands.[12,17] The calculations were performed both in vacuum and in solvent. Solvent effects were simulated by embedding a system in a conductor polarizable continuum medium (CPCM) with an appropriate dielectric constant as implemented in the Gaussian 09 code.[18] Acetonitrile (CH_3CN with dielectric constant

Scheme 1. Ru−Polypyridine Complexes Used in the Present Work[a]

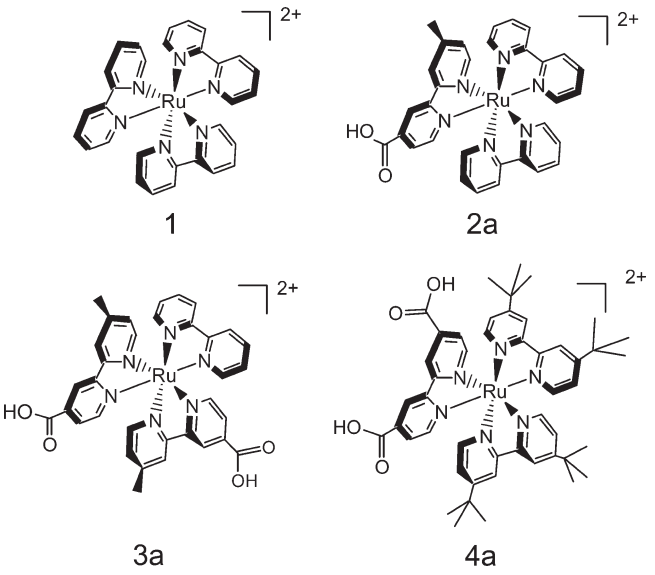

[a] Only the protonated forms of complexes **2**, **3**, and **4** are shown. The fully deprotonated forms of the complexes are referred to in text as **2b**, **3b**, and **4b**.

36.64) was chosen as a reference solvent for consistency with the experimental studies.

RESULTS AND DISCUSSION

A. FTIR Spectroscopy. Recently, McQuillan and others have demonstrated that the process of the ligand exchange on the surface of CdSe NCs could be studied *in situ* by ATR-FTIR, whereby a thin film of NCs is used to model the surface of individual NCs in solution.[19] In the present work we use a similar approach to investigate the coupling of the Ru−polypyridine complex to the surface of the CdSe NC. The approach is schematically shown in Figure 1a. We examine not only the structural changes taking place at the NC film−solution interface but also the influence of the number of the anchoring carboxylic groups on the efficiency of the chemical coupling. For this purpose four different Ru−polypyridine complexes were prepared: complex **1**, which does not have any anchoring groups (a control); complex **2** having one carboxylic group on one of the bipyridine ligands; complex **3** bearing two bipyridine ligands each with one carboxylic acid; and complex **4** having two anchoring groups on a single bipyridine ligand (Scheme 1). In the experiment the films were exposed to a 10^{-3} M solution of a complex in acetonitrile. The choice of the solvent was motivated by high solubility of the complexes and low solubility of the CdSe NCs. The spectrum recorded immediately upon addition of a complex solution was used as background.

Figure 1b shows the time evolution of ATR-FTIR spectra of a deposited TOPO-capped CdSe NC film exposed to a 10^{-3} M solution of complex **1** in acetonitrile. Also shown are the spectra of the independently prepared films of CdSe NCs and of complex **1**. As can be seen in the figure, within minutes of the CdSe NC film exposure to the solution of the complex, characteristic spectral features of the complex are detected. Most notable is the band at 1606 cm^{-1} and the triplet of bands in the region

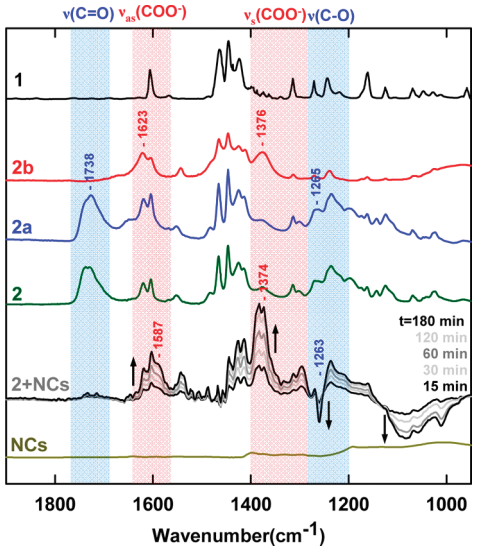

Figure 2. ATR-FTIR spectra observed following exposure of CdSe NC film to 10^{-3} M acetonitrile solution of complex **2** (**2** + NCs). The spectra shown are a difference between the spectrum recorded at indicated delay and the spectrum recorded immediately upon exposure of the NC film of the complex. Also shown are the spectra of independently prepared films comprising complexes **1**, and **2** and its protonated (**2a**) and deprotonated (**2b**) forms and the film of NCs, measured as dry films.

1420−1470 cm^{-1} assigned to bipyridine ring stretching modes.[20] In the high frequency region, 2800−3200 cm^{-1}, a strong negative feature is observed, attributed to a loss of TOPO ligand from the NC surface.[19] In our studies the solution containing the complex was static, rather than flown over the NC film. Therefore, the negative feature appears as a result of diffusion of the ligand away from the NC film surface and its subsequent dilution. No significant changes in peak positions or intensities were observed with further exposure. Since we do not detect any spectral shifts when comparing the spectrum of **1** + NC with the spectrum of the independently prepared film of **1**, we conclude that the features observed in the medium frequency range are due to a small amount of complex physisorbed within the pores of the NC film. This is consistent with the result of our recent photoluminescence studies, which showed no evidence of chemical interaction between complex **1** and CdSe NCs in solution.[5] As discussed below, the results are distinctly different when the NC film is exposed to solution of complexes **2** and **3**.

The time evolution of an ATR-FTIR spectrum of the NC film exposed to the solution of the complex **2** is shown in Figure 2. Also shown are the spectra of the NC film without **2** present and an independently prepared film of complex **2**. To assist in interpretation of spectral changes in the mixture, spectra of films of the fully protonated **2a** and fully deprotonated **2b** versions of the complex **2** are also shown (here and later **a** and **b** are used to distinguish the protonated (**a**) and deprotonated (**b**) forms of the Ru complexes). The complexes **2a** and **2b** were prepared by addition of HPF_6 or NaOH to the acetonitrile solution of the complex as described in the Experimental Section. In Figure 2 the fingerprint regions for the protonated and deprotonated form of the carboxylic acid are shaded in blue and red, respectively.[21]

Referring to the ATR-FTIR time-evolution spectrum of **2** + NC shown in Figure 2, we make the following observations:

dx.doi.org/10.1021/la200531s |*Langmuir* 2011, 27, 8377–8383

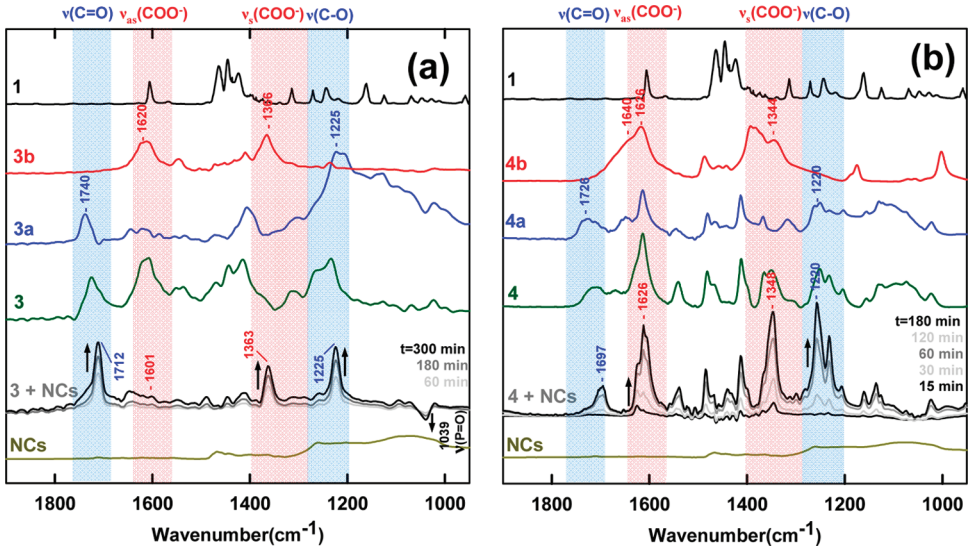

Figure 3. (a) ATR-FTIR spectra observed following exposure of CdSe NC film to 10^{-3} M acetonitrile solution of complex **3** (**3** + NCs). The spectra shown are a difference between the spectrum recorded at indicated delay and the spectrum recorded immediately upon exposure of the NC film to the solution of the complex. Also shown are the spectra of independently prepared films comprising complexes **1** and **3** and their fully protonated (**3a**) and deprotonated (**3b**) forms and the film of NCs. (b) Results of the same experiment as in (a), but for complex **4**.

Within the first 15 min of exposure of the NC film to a solution containing the complex, several spectral features consistent with the presence of the complex adsorbed at the NC film surface are detected. These features are distinctly different from the spectrum of an independently prepared film of **2**. Specifically, the ν(C═O) characteristic band at 1738 cm^{-1} clearly visible in the spectra of **2** and **2a** is lacking in the spectrum of **2** + NC. The band at 1265 cm^{-1} in the spectra of **2** and **2a**, which we assign to the ν(C−O) stretching mode of the carboxylic acid, is observed as a negative feature in the spectrum of **2** + NC. In addition, a dominant feature at 1374 cm^{-1}, visible in the spectrum of **2** + NC, is not detected in the spectrum of **2** or **2a**. Interestingly, a similar feature peak is detected in the spectrum of **2b**, where it is attributable to the symmetric stretch of the deprotonated carboxylic acid group $\nu_s(COO^-)$. A series of bands in the regions 1420−1470 and 1600−1630 cm^{-1} correspond to the bipyridine ring stretching vibrations. However, compared to the spectrum of **2**, the relative intensities of these bands are distinctly different and small shifts to lower energies are detected for the case of **2** + NC. Moreover, a new feature at ∼1587 cm^{-1} is detected as a shoulder in the **2** + NC spectrum.

We interpret the above observations as follows. The disappearance of the ν(C═O) and ν(C−O) bands associated with the stretching vibrations of the carboxylic acid group and emergence of a band at 1374 cm^{-1} associated with the $\nu_s(COO^-)$ vibration are consistent with the formation of the deprotonated form of the carboxylic acid. Therefore, we conclude that the interaction between complex **2** (shown as protonated in Figure 2) and the CdSe NC film leads to the deprotonation of the complex. This is an expected result of chemical attachment of the complex to the surface of the NCs. Deprotonation of the carboxylic acid group upon adsorption onto the NC surface was observed previously[19] and is consistent with recent results of our photoluminescence studies,[5] in which deprotonation was detected as a shift of the complex emission to higher energy. The changes in the relative intensities of the bands associated with bipyridine ring stretching vibrations also support the conclusion that the complex is chemically bound to the NC surface. Consistent with this interpretation, we attribute the appearance of the new distinct shoulder at 1587 cm^{-1} to the asymmetric stretch $\nu_{as}(COO^-)$ of the deprotonated carboxylic acid group. It is shifted from 1623 cm^{-1} observed in the spectrum of the deprotonated complex **2b** due to a strong chemical interaction between NC surface and the complex. The fact that the ν(C−O) stretching frequency of the carboxylic acid at 1265 cm^{-1} is observed as a negative feature in the spectrum of **2** + NC suggests, that, at least for fraction of the complexes the adsorption of the complex precedes the deprotonation step.

Figure 3a shows the ATR-FTIR spectra of the CdSe NC film following exposure to complex **3**. The spectra can be interpreted similarly to complex **2**, but there are few notable differences. First, the ν(C═O) stretch feature that is not observed in the **2** + NC spectrum is clearly visible in the spectrum of **3** + NC. This feature at 1712 cm^{-1} is red-shifted compared to complex **3a**, where it is observed at 1740 cm^{-1}. Second, the band associated with the ν(C−O) stretch of the carboxylic group that was observed as a negative feature at 1263 cm^{-1} in the spectrum of **2** + NC is detected as a positive feature at 1226 cm^{-1} in **3** + NC. Similar to the case of the **2** + NC the band at 1363 cm^{-1} is assigned to the symmetric stretch, $\nu_s(COO^-)$, of the deprotonated carboxylic acid. The presence of two types of bands associated with C═O, C−O, and COO^- vibrations can be explained by the presence of two types of carboxylic groups on the complex: one is protonated and another is deprotonated. In the complex **3**, which is initially essentially fully protonated, one of the carboxylic acid groups functions as an anchor to the NC surface and is deprotonated as a result of adsorption, as observed in the case of the complex **2**. However, the second carboxylic acid group, which is oriented away from the NC surface, functions as a "spectrator" group and is not involved in the complex-to-NC chemical binding. This carboxyl group remains protonated. As a result of the binding to the NC surface, the electronic structure of the complex is distorted, which is reflected in the shifts of the bands associated with the "spectrator" carboxylic acid to the

dx.doi.org/10.1021/la200531s |*Langmuir* 2011, 27, 8377–8383

Scheme 2. Possible Modes of Attachement of the Carboxylic Acids to Semiconductor Surfaces and Corresponding Difference in Frequencies of Symmetric and Asymmetric Stretches of the Carboxylic Acid Group[a]

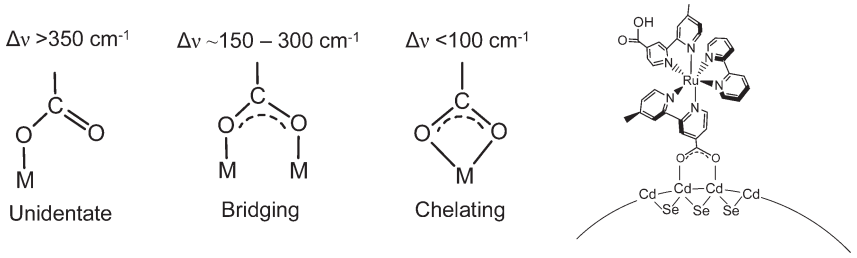

[a] The figure on the right shows the proposed mode of coupling of the Ru−polypyridine complexes to the surface of CdSe NCs.

Table 1. Assignments of the Spectral Features Associated with the Vibrational Frequencies (cm^{-1}) of Carboxylic Groups of the Functionalized Ru−Polypyridine Complexes in Solution and upon Exposure to the Film of TOPO-Capped CdSe NCs

assignment	2a	2b	2−NC	3a	3b	3−NC	4a	4b	4−NC
ν(C═O)	1738			1740			1726		
$\nu(C{=}O)_{ads}$						1712			1697
ν(C−O)	1265			1225		1225		1626 1640	1626
$\nu_{as}(COO^-)$		1623	1587		1620	1601		1344	1348
$\nu_s(COO^-)$		1376	1374		1366	1363	1220		1220
$\Delta\nu = \nu_{as} - \nu_s$		245	213		254	238		296	278

lower energies. Using this interpretation, we assign the positive features at 1712 and at 1226 cm^{-1} to the ν(C═O) and ν(C−O) stretches of the "spectrator" group, respectively.

A similar picture was observed for the NC film exposed to the solution of the complex **4** (Figure 3b). As in case of complex **3** the spectral changes are consistent with the presence of two types of carboxyl groups: the deprotonated anchoring group and protonated "spectrator" group. Specifically, the ν(C═O) stretch feature of the protonated "spectrator" group is observed in the **4** + NC spectrum at 1697 cm^{-1} and is shifted by ~29 cm^{-1} to a lower energy compared to the corresponding band in the spectrum of **4a.** The ν(C−O) stretch of the same group is detected as a positive feature at 1220 cm^{-1}. The $\nu_s(COO^-)$ of the surface bound carboxylate group is observed at 1348 cm^{-1}.

The analysis of the IR spectral features associated with the carboxyl groups allows determination of the binding mode of the complexes **2a**, **3a**, and **4a** to the NC surface. As was shown previously,[22] the separation, $\Delta\nu = \Delta\nu_{as} - \Delta\nu_s$, between the asymmetric and symmetric stretch of the carboxylate group can by used as an empirical guideline for distinguishing between unidentate, bridging, and chelating binding modes (see Scheme 2). This approach was previously used effectively in determination of the binding mode of carboxylic acids to various metal oxide surfaces[21] as well as in determination of the mode of attachment of the functionalized Ru−polypyridine complexes to the surfaces of metal oxides and glass.[23] The relevant data for the complexes studied here, based on results shown in Figures 2 and 3, are summarized in Table 1. For all complexes, the values of $\Delta\nu$ = 200−250 cm^{-1} are very similar to the values observed for the deprotonated version of the complexes, which is consistent with a symmetric mode of attachment via a bridging mode (see Scheme 2).[21,22]

B. Theoretical Studies. Because of the symmetry of the crystal facets, the NC surface has several distinct sites, schematically marked as A−D in Figure 4, where an organic ligand can bind to the surface of the $Cd_{33}Se_{33}$. Positions A_1 and C correspond to the Cd atoms on the surface that are bound to only two Se atoms and have two unsaturated valences. Positions A_2, B, and D correspond to Cd atoms that are bound to three Se atoms, having one unsaturated valence bond. Our previous computational studies[17] have shown that Cd atoms bound to only two Se atoms are chemically more active, resulting in a stronger interaction between ligands, compared to Cd atoms bound to three Se atoms. Therefore, in the starting geometry of the optimization the ligand was positioned close to the Cd atoms in the A_1 or C positions of the nonoptimized $Cd_{33}Se_{33}$ bulk-like structure, and the system was allowed to relax to its optimal geometry.

Gas-Phase Calculations. On the basis of the calculated binding energies, E_b, of the geometry optimized NC−acetate assemblies in vacuum, with geometry optimization initiated from different starting configurations (bidentate, bridging, or chelating), we conclude that the bridging mode is the energetically most favorable mode of surface attachment (see Table 2). When the simulation was initiated with the acetate in the unidentate position, in several cases we observed that the acetate shifted to the chelating or bridging binding configuration during geometry optimization. Consequently, we conclude that the unidentate attachment is energetically unfavorable. This is consistent with the experimental observations summarized in the previous section. In contrast, for the acetic acid (CH_3COOH), the binding to the $Cd_{33}Se_{33}$ surface occurs only in the unidentate position. However, the binding energy of the NC−acetic acid assembly is significantly smaller than the binding energy of the NC−acetate anion assembly (see Table 2). The difference of ~3 eV between binding energies of the protonated and deprotonated forms of carboxylic acid points to a greater probability of anchoring the ligand to the surface when the ligand is deprotonated, which is consistent with the experimental results.

For the acetate, the change in binding energies between bridging and chelating modes calculated in vacuum is also

substantial and varies from 0.5 to 1.5 eV (positions A−C, Figure 4). Interestingly, the large binding energy of the bridging attachment does not necessarily correspond to equal bond lengths between the Cd atoms and two oxygen atoms of the acetate. For example, the Cd−O bonds differ by 0.27 Å in the bridging A_1-A_2 attachment (Table 2). Despite this asymmetry of the Cd−O bonds, the C−O bonds of the acetate still have a significant resonance character, so that the difference between the symmetric and asymmetric C−O vibrational frequencies is expected to be typical of bridging configurations.

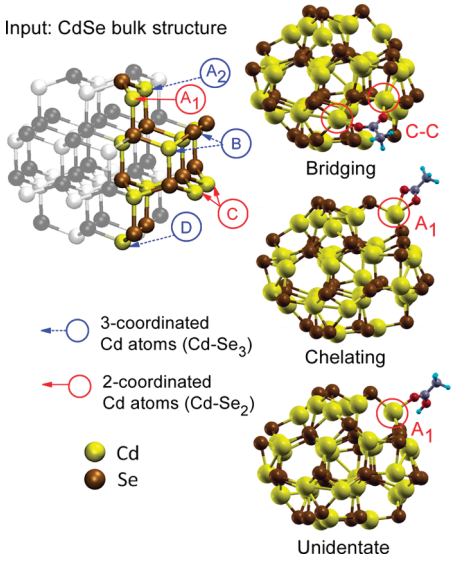

Figure 4. Structures of the simulated $Cd_{33}Se_{33}$ NC and adsorbed -acetate and acetic acid groups. The left panel shows the $Cd_{33}Se_{33}$ construction from the ideal CdSe bulk crystal. Surface Cd atoms lacking two nearest neighbors are marked as A_1 and C (red); 3-coordinated atoms are marked as A_2, B, and D (blue). The right panel represents optimized geometries of the $Cd_{33}Se_{33}$ with the acetate ion attached in the chelating or bridging mode and acetic acid molecule attached in unidentate mode, as has been obtained from DFT calculations using B3LYP functional and LANL2DZ basis set. Calculations are done in CH_3CN solution based on CPCM-GAUSSIAN-09 solvent model.

Calculations in the Presence of Solvent. Addition of the solvent model to the calculations leads to more symmetric Cd−O bonds in the bridging configuration of the NC−acetate assembly for all nonequivalent sites. In contrast, solvent distorts the symmetry of the Cd−O bond in the chelating mode, resulting in a significantly longer Cd−O bond for one of the oxygen atoms (∼2.5−2.6 Å, Table 2). This gives the chelating structures a partial unidentate character. Therefore, vibrational frequencies of the C−O bonds of a carboxylate group anchoring to the CdSe via the bridging mode are expected to be distinctly different from those of the chelate and unidentate binding.

In addition, we note that in the presence of solvent an increase in the HOMO−LUMO band gap was observed for all systems (see Table 2). All structures simulated in solvent had an energy gap of ∼3 eV, which fortuitously agrees well with the lowest absorption peak (∼2.99 eV) experimentally observed and assigned to the $Cd_{33}Se_{33}$ NCs.[14,15] This result provides support for the suitability of the computational methodology used in the present work. Independent of the binding mode, calculations performed in the presence of solvent lead to a significant decrease of the binding energy values in all cases, indicating that the dielectric environment effects are critical for quantitative evaluation of the binding energies. The overall trend of ligand−NC interactions with respect to the ligand attachment remains the same as in vacuum: attachment to the bridging binding sites is characterized with the largest binding energies ∼0.6−0.8 eV, while unidentate binding of the protonated carboxyl group corresponds to the weakest interaction of ∼0.2 eV. In solvent, the difference in binding energy between the bridging and chelating configurations is ∼0.1 eV, which is roughly 1 order of magnitude smaller than the value calculated in vacuum. Nonetheless, this difference is much higher than the room temperature thermal fluctuations, which indicates a higher stability of the bridging configuration, consistent with the conclusion of the experimental studies. Although the direct comparison of the calculated binding energies with experimental data in the systems studied here is unavailable, we note that the values shown in Table 2 are of the same order as, for example, experimentally determined binding energies of acrylic acid adsorbed on the $CuO_2(100)$ surface (∼0.66 eV)[24] and acetic and fluorinated acids adsorbed on Ag (111) surfaces (0.45 and 0.59 eV, respectively).[25] These results suggest feasibility of preparing stable

Table 2. Calculated Binding Energies, Band Gaps, and Cd−O Bond Lengths of the $Cd_{33}Se_{33}$ NC with the Adsorbed Acetate (CH_3COO^-) and Acetic Acid (CH_3COOH) Groups in Vacuum and in CH_3CN Solvent (Shown in Parentheses) Using B3LYP Functional and LANL2DZ Basis Set

		energy (eV)		bond length (Å)	
binding mode	ligand position	E_{bind}	E_{gap}	Cd−O(1)	Cd−O(2)
bridging CH_3COO^-	A_1-A_2	−4.5 (−0.8)	2.78 (3.04)	2.19 (2.31)	2.46 (2.32)
	A_1-B	−4.3 (−0.6)	2.53 (2.98)	2.21 (2.31)	2.25 (2.34)
	C_1-C_2	−4.4 (−0.7)	2.20 (3.14)	2.19 (2.31)	2.20 (2.33)
chelating CH_3COO^-	A_1	−3.8 (−0.5)	2.66 (3.02)	2.30 (2.39)	2.38 (2.62)
	C_1	−3.7 (−0.5)	2.14 (2.96)	2.33 (2.44)	2.35 (2.53)
	C_2	−3.0 (−0.3)[a]	2.01 (3.17)[a]	2.30	2.40
unidentate CH_3COOH	A_1	−0.9 (−0.2)[a]	2.56 (3.22)[a]	2.30	3.85
	C_1	−1.0	2.51	2.37	3.75
	C_2	−0.7	2.45	2.31	3.93

[a] Values were obtained using geometries optimized in vacuum, while the electronic structure is calculated in CH_3CN based on CPCM-GAUSSIAN-09 solvent model.

dx.doi.org/10.1021/la200531s |*Langmuir* 2011, 27, 8377–8383

NC−complex assemblies via a ligand exchange process. More detailed studies of the NC surface exchange equilibrium in the presence of complex **4a** are presented in ref 5.

CONCLUSIONS

In this study we have demonstrated that combination of ATR-FTIR studies and DFT theoretical modeling can provide important insights about the mechanism of attachment of functionalized Ru−polypyridine complexes to the surface of CdSe NCs. We showed that when a film of NCs is exposed to a solution of a complex lacking an anchoring functional group, the complex can diffuse into the pores of the film and physisorb onto the NC surface. In this case we see no evidence of chemical interaction between the complexes and the NCs. However, when the NC film is exposed to the Ru−polypyridine complexes functionalized with a carboxylic acid group, the complexes chemically couple to the NC surface, and the anchoring carboxylic acid group is deprotonated in the process. For the complexes containing two carboxylic acid groups, one of the groups functions as an anchoring group and is deprotonated as a result of the adsorption process, while the second group, a "spectrator", remains protonated. The observed energy difference between the symmetric and asymmetric stretches of the deprotonated carboxylic acid group suggests that the complexes are bound to the NC surface in the bridging mode configuration. The results of DFT modeling are consistent with the experiment. They reveal that the complexes bind exclusively to the Cd atoms and that for carboxylate the bridging mode is the energetically most favorable mode of attachment for all nonequivalent NC surface sites. The attachment of a carboxylic acid is thermodynamically less favorable by ∼3 eV.

AUTHOR INFORMATION

Corresponding Author
*E-mail: sykoram@lanl.gov.

ACKNOWLEDGMENT

A.Y.K., M.S., S.K. and V.A. acknowledge support of the Los Alamos Directed Research and Development funds. E.B. and S.T. acknowledge support of the Center for Advanced Solar Photophysics, an Energy Frontier Research Center funded by the U.S. Department of Energy (DOE), Office of Science (OS), Office of Basic Energy Sciences (BES). T.C. and T.J.M. acknowledge funding by the Chemical Sciences, Geosciences and Biosciences Division of the Office of Basic Energy Sciences, U.S. Department of Energy, through Grant DE-FG02-06ER15788.

REFERENCES

(1) (a) Burda, C.; Chen, X.; Narayanan, R.; El-Sayed, M. A. *Chem. Rev.* **2005**, *105* (4), 1025–1102. (b) Regulacio, M. D.; Han, M.-Y. *Acc. Chem. Res.* **2010**, *43* (5), 621–630. (c) Smith, A. M.; Nie, S. *Acc. Chem. Res.* **2010**, *43* (2), 190–200.

(2) Talapin, D. V.; Lee, J.-S.; Kovalenko, M. V.; Shevchenko, E. V. *Chem. Rev.* **2009**, *110* (1), 389–458.

(3) Callan, J.; Mulrooney, R.; Kamila, S.; McCaughan, B. *J. Fluoresc.* **2008**, *18* (2), 527–532.

(4) (a) Nann, T.; Ibrahim, S. K.; Woi, P.-M.; Xu, S.; et al. *Angew. Chem., Int. Ed.* **2010**, *49* (9), 1574–1577. (b) Sykora, M.; Petruska, M. A.; Alstrum-Acevedo, J.; Bezel, I.; et al. *J. Am. Chem. Soc.* **2006**, *128* (31), 9984–9985.

(5) Koposov, A. Y.; Szymanski, P. L.; Cardolaccia, T.; Meyer, T. J., et al. *Adv. Funct. Mat.,* in press.

(6) McQuillan, A. J. *Adv. Mater.* **2001**, *13* (12−13), 1034–1038.

(7) Kilina, S.; Ivanov, S.; Tretiak, S. *J. Am. Chem. Soc.* **2009**, *131* (22), 7717–7726.

(8) Takeuchi, K. J.; Thompson, M. S.; Pipes, D. W.; Meyer, T. J. *Inorg. Chem.* **1984**, *23* (13), 1845–1851.

(9) Peek, B. M.; Ross, G. T.; Edwards, S. W.; Meyer, G. J.; et al. *Int. J. Pept. Protein Res.* **1991**, *38* (2), 114–123.

(10) Yu, W. W.; Qu, L. H.; Guo, W. Z.; Peng, X. G. *Chem. Mater.* **2003**, *15* (14), 2854–2860.

(11) Murray, C. B.; Norris, D. J.; Bawendi, M. G. *J. Am. Chem. Soc.* **1993**, *115* (19), 8706–8715.

(12) Yang, P.; Tretiak, S.; Masunov, A. E.; Ivanov, S. *J. Chem. Phys.* **2008**, *129* (7), 074709.

(13) Rempel, J. Y.; Trout, B. L.; Bawendi, M. G.; Jensen, K. F. *J. Phys. Chem. B* **2006**, *110* (36), 18007–18016.

(14) Kasuya, A.; Sivamohan, R.; Barnakov, Y. A.; Dmitruk, I. M.; et al. *Nature Mater.* **2004**, *3* (2), 99–102.

(15) (a) Pedersen, J.; Bjornholm, S.; Borggreen, J.; Hansen, K.; et al. *Nature* **1991**, *353* (6346), 733–735. (b) Evans, C. M.; Guo, L.; Peterson, J. J.; Maccagnano-Zacher, S.; et al. *Nano Lett.* **2008**, *8* (9), 2896–2899.

(16) Frisch, M. J.; Trucks, G. W.; Schlegel, H. B.; Scuseria, G. E.; et al. *Gaussian 09, Revision A.1*; Gaussian, Inc.: Wallingford, CT, 2009.

(17) Kilina, S.; Batista, E. R.; Yang, P.; Tretiak, S.; et al. *ACS Nano* **2008**, *2* (7), 1381–1388.

(18) (a) Barone, V.; Cossi, M.; Tomasi, J. *J. Comput. Chem.* **1998**, *19* (4), 404–417. (b) Cossi, M.; Barone, V.; Mennucci, B.; Tomasi, J. *Chem. Phys. Lett.* **1998**, *286* (3−4), 253–260. (c) Cossi, M.; Rega, N.; Scalmani, G.; Barone, V. *J. Comput. Chem.* **2003**, *24* (6), 669–681.

(19) Young, A. G.; Al-Salim, N.; Green, D. P.; McQuillan, A. J. *Langmuir* **2008**, *24* (8), 3841–3849.

(20) Omberg, K. M.; Schoonover, J. R.; Treadway, J. A.; Leasure, R. M.; et al. *J. Am. Chem. Soc.* **1997**, *119* (30), 7013–7018.

(21) (a) Dobson, K. D.; McQuillan, A. J. *Spectrochim. Acta, Part A* **1999**, *55* (7−8), 1395–1405. (b) Dobson, K. D.; McQuillan, A. J. *Spectrochim. Acta, Part A* **2000**, *56* (3), 557–565.

(22) Deacon, G. B.; Phillips, R. J. *Coord. Chem. Rev.* **1980**, *33* (3), 227–250.

(23) (a) Meyer, T. J.; Meyer, G. J.; Pfennig, B. W.; Schoonover, J. R.; et al. *Inorg. Chem.* **1994**, *33* (18), 3952–3964. (b) Finnie, K. S.; Bartlett, J. R.; Woolfrey, J. L. *Langmuir* **1998**, *14* (10), 2744–2749.

(24) Schulz, K. H.; Cox, D. F. *J. Phys. Chem.* **1992**, *96* (18), 7394–7398.

(25) Parker, B.; Immaraporn, B.; Gellman, A. J. *Langmuir* **2001**, *17* (21), 6638–6646.